Project Report
ATC-416

Secondary Surveillance Phased Array Radar (SSPAR): Initial Feasibility Study

M.E. Weber
M.L. Wood
J.R. Franz
D. Conway
J.Y.N. Cho

6 February 2014

Lincoln Laboratory
MASSACHUSETTS INSTITUTE OF TECHNOLOGY
LEXINGTON, MASSACHUSETTS

Prepared for the Federal Aviation Administration,
Washington, D.C. 20591

This document is available to the public through
the National Technical Information Service,
Springfield, Virginia 22161

TECHNICAL REPORT STANDARD TITLE PAGE

1. Report No.	2. Government Accession No.	3. Recipient's Catalog No.
ATC-416		

4. Title and Subtitle	5. Report Date
Secondary Surveillance Phased Array Radar (SSPAR): Initial Feasbility Study	6 February 2014
	6. Performing Organization Code

7. Author(s)	8. Performing Organization Report No.
M.E. Weber, M.L. Wood, J.R. Franz, D. Conway, and J.Y. N. Cho, MIT Lincoln Laboratory	ATC-416

9. Performing Organization Name and Address	10. Work Unit No. (TRAIS)
MIT Lincoln Laboratory 244 Wood Street Lexington, MA 02420-9108	11. Contract or Grant No. FA8721-05-C-0002

12. Sponsoring Agency Name and Address	13. Type of Report and Period Covered
Department of Transportation Federal Aviation Administration 800 Independence Ave., S.W. Washington, DC 20591	Project Report
	14. Sponsoring Agency Code

15. Supplementary Notes

This report is based on studies performed at Lincoln Laboratory, a federally funded research and development center operated by Massachusetts Institute of Technology, under Air Force Contract FA8721-05-C-0002.

16. Abstract

The U.S. Federal Aviation Administration is deploying Automatic Dependent Surveillance-Broadcast (ADS-B) to provide next-generation surveillance derived through down- and cross-link of global positioning satellite (GPS) navigation data. While ADS-B will be the primary future surveillance system, FAA recognizes that backup surveillance capabilities must be provided to assure that air traffic control (ATC) services can continue to be provided when individual aircraft transponders fail and during localized, short-duration GPS outages. This report describes a potential ADS-B backup capability, Secondary Surveillance Phased Array Radar or SSPAR. SSPAR will interrogate aircraft transponders and receive replies using a sparse, non-rotating array of approximately 17 omnidirectional (in azimuth) antennae. Each array element will transmit and receive independently so as to form directional transmit beams for transponder interrogation, and support high-resolution direction finding for received signals. Because each SSPAR element is independently digitized, transponder returns from all azimuths can be continuously monitored. Thus SSPAR can exploit the spontaneous "squitters" emitted by aircraft equipped with Traffic Alert and Collision Avoidance System (TCAS) and ADS-B avionics to reduce spectrum usage and maintain the high surveillance update rate (~1 per second) achieved by ADS-B. Recurring costs for SSPAR will be low since it involves no moving parts and the number of array channels is small.

This report describes an SSPAR configuration supporting terminal operations. We consider interrogation and receive approaches, antenna array configuration, signal processing and preliminary performance analysis. An analysis of SSPAR's impact on spectrum congestion in the beacon radar band is presented, as are concepts for integrating SSPAR and next generation primary radar to improve the efficiency and accuracy of aircraft and weather surveillance.

17. Key Words	18. Distribution Statement
	This document is available to the public through the National Technical Information Service, Springfield, VA 22161.

19. Security Classif. (of this report)	20. Security Classif. (of this page)	21. No. of Pages	22. Price
Unclassified	Unclassified	54	

This page intentionally left blank.

EXECUTIVE SUMMARY

The U.S. Federal Aviation Administration is deploying Automatic Dependent Surveillance-Broadcast (ADS-B) to provide next-generation surveillance derived through down- and cross-link of global positioning satellite (GPS) navigation data. While ADS-B will be the primary future surveillance system, FAA recognizes that backup surveillance capabilities must be provided to assure that air traffic control (ATC) services can continue to be provided when individual aircraft transponders fail and during localized, short-duration GPS outages. This report describes a potential ADS-B backup capability, Secondary Surveillance Phased Array Radar or SSPAR. SSPAR will interrogate aircraft transponders and receive replies using a sparse, non-rotating array of approximately 17 omnidirectional (in azimuth) antennae. Each array element will transmit and receive independently so as to form directional transmit beams for transponder interrogation, and support high-resolution direction finding for received signals. Because each SSPAR element is independently digitized, transponder returns from all azimuths can be continuously monitored. Thus SSPAR can exploit the spontaneous "squitters" emitted by aircraft equipped with Traffic Alert and Collision Avoidance System (TCAS) and ADS-B avionics to reduce spectrum usage and maintain the high surveillance update rate (~1 per second) achieved by ADS-B. Recurring costs for SSPAR will be low since it involves no moving parts and the number of array channels is small.

This report describes an SSPAR configuration supporting terminal operations. We consider interrogation and receive approaches, antenna array configuration, signal processing and preliminary performance analysis. An analysis of SSPAR's impact on spectrum congestion in the beacon radar band is presented, as are concepts for integrating SSPAR and next generation primary radar to improve the efficiency and accuracy of aircraft and weather surveillance.

This page intentionally left blank.

TABLE OF CONTENTS

This page intentionally left blank.

LIST OF ILLUSTRATIONS

LIST OF ILLUSTRATIONS
(Continued)

LIST OF TABLES

This page intentionally left blank.

1. INTRODUCTION

An important component of the Federal Aviation Administration's (FAA) Next Generation Air Transportation System (NextGen) is high quality, aircraft position and intent information provided through down- and cross-link of Global Positioning Satellite (GPS) navigation data. This capability will be realized through the FAA's Automatic Dependent Surveillance-Broadcast (ADS-B) program. Deployment of more than 700 ADS-B ground-stations is largely complete, and aircraft equipage with compatible avionics is mandated by 2020. While ADS-B will be the primary future surveillance system, FAA recognizes that backup surveillance capabilities must be provided to assure that air traffic control (ATC) services can continue to be provided when individual aircraft transponders fail and during localized, short-duration GPS outages.

To mitigate single-aircraft avionics failures, FAA will retain existing "primary" (skin-paint) radars such as Airport Surveillance Radars (ASR) in the short and midterm. A "NextGen Surveillance and Weather Radar Capability (NSWRC)" program has been initiated to develop long-term alternatives for future primary radar services that range from procurement of additional legacy radar systems to replacement of current radar networks with multifunction phased array radar (MPAR). Existing "secondary" (transponder-based) radars will also be retained to support ATC services without loss of capacity during a GPS outage. All en route beacon radars and terminal beacons at the busiest 43 airports will be retained in the short and midterm. A "NextGen Backup Surveillance Capability (NBSC)" program will evaluate longer-term cooperative surveillance backup alternatives, including procurement of replacement beacon radar systems and wide-area multilateration (WAM). The NSWRC and NBSC programs are scheduled to implement next-generation primary and cooperative surveillance systems beginning in 2023.

In this report, we discuss an alternative for the NBSC program that we have dubbed Secondary Surveillance Phased Array Radar or SSPAR. SSPAR extends previous concepts for low-cost, transponder based ATC surveillance (Harman and Wood, 2011) by exploiting advanced array design and processing concepts developed in the signals intelligence (SIGINT) community (e.g., Hatke, 1997). Figure 1-1 depicts the SSPAR antenna array, mounted on the frustum of a Terminal MPAR (Weber et al., 2013). This sparse array will consist of approximately 17 elements, situated along the circumference of a 4 m diameter circle. Each array element will transmit and receive independently so as to form directional (approximately 4^o in azimuth) transmit beams for transponder interrogation, and support high-resolution direction finding for received signals. Preliminary analysis indicates that the conceptual SSPAR array configuration will support the 1 milliradian (0.05^o) azimuth accuracy for transponder replies that is achieved by current monopulse secondary radars. Because each SSPAR element is independently digitized, transponder returns from all azimuths can be continuously monitored. Thus SSPAR can exploit the spontaneous "squitters" emitted by aircraft equipped with Traffic Alert and Collision Avoidance System (TCAS) and ADS-B avionics. As described subsequently, this will reduce spectrum congestion in the 1030/1090 MHz frequency band used for beacon interrogation/reply, and will maintain the high surveillance update rate (~1 per second) achieved by ADS-B. (Current terminal and en route beacon

radars rotate respectively at 12 and 5 revolutions per minute, which may constrain certain NextGen procedures such as closely spaced parallel runway operations.) Finally, the recurring costs for SSPAR will be low since it involves no moving parts and the number of array channels is small.

Figure 1-1. SSPAR array mounted on frustum of Terminal MPAR.

In this report, we describe in detail an SSPAR configuration supporting terminal operations. The concepts and analysis are readily extensible to a longer-range sensor for en route surveillance, requiring simply that a larger antenna array be used. Section 2 describes the concept of operations for SSPAR, including interrogation and receive approaches for both Mode-Select (Mode-S) and Air Traffic Control Radar Beacon System (ATCRBS)–equipped aircraft. Section 3 discusses the SSPAR antenna configuration and signal processing approaches, and presents preliminary performance modeling results. In Section 4, we describe a candidate system configuration and develop initial recurring costs estimates based on appropriate commercial-off-the-shelf (COTS) components. An analysis of SSPAR's impact on spectrum congestion in the beacon radar band is presented in Section 5. Finally, in Section 6 we discuss concepts for integrating SSPAR and primary radar (e.g., MPAR) to improve the efficiency and accuracy of aircraft and weather surveillance.

2. SSPAR INTERROGATION/RECEIVE CONCEPT OF OPERATIONS

2.1 LEGACY BEACON RADAR SYSTEMS

Since SSPAR performance goals are based on existing monopulse and Mode-S secondary surveillance radar (SSR), and interrogation/receive strategies are derived from both SSR and TCAS, it is useful to briefly describe these systems. The current Mode-S terminal antenna (Figure 2-1) is a rotating, planar dipole array 26 feet wide, consisting of 35 columns with 10 dipoles in each column. The array elements are phased so as to produce "sum" and "difference" azimuth patterns, from which transponder direction can be determined to 1 milliradian accuracy using monopulse. A "sidelobe suppression" (SLS) pulse is transmitted from a colocated omnidirectional antenna so that aircraft outside the main beam of the radar will not respond to interrogations. The sensor continuously sends Mode-S "All Call" interrogations to which untracked aircraft reply with their 24-bit unique Mode-S address. Once that address is learned, a track is formed and subsequently updated every scan using "Roll Call" interrogations addressed to the individual transponders. Mode-S was designed to acquire and track ATCRBS–equipped aircraft using a separate interrogation to which Mode-S–equipped aircraft will not respond. However, an incompatibility in one manufacturer's (Terra) ATCRBS transponder currently prevents this feature from being used.

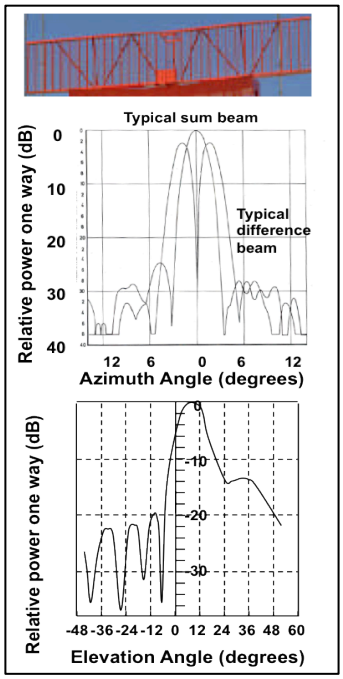

Figure 2-1. Mode-S dipole array (top), azimuth sum and difference patterns (middle), and elevation pattern (bottom).

TCAS uses a different acquisition strategy since TCAS antennae are small, generating four very broad beams as illustrated in Figure 2-2. With such broad beams, use of an All Call interrogation to acquire untracked Mode-S transponders would be problematic because many replies would come back and garble each other. Instead, the Mode-S transponder has been designed to emit All Call replies spontaneously once per second. TCAS monitors these "squitters" and when it receives one from a previously unknown transponder, it begins tracking this aircraft using Roll Call interrogations. For surveillance of ATCRBS–equipped aircraft, TCAS uses a sequence of "Whisper-Shout" interrogations (described below) from each of its beams, thereby reducing the likelihood that overlapping replies from multiple aircraft will be received in response to any single interrogation.

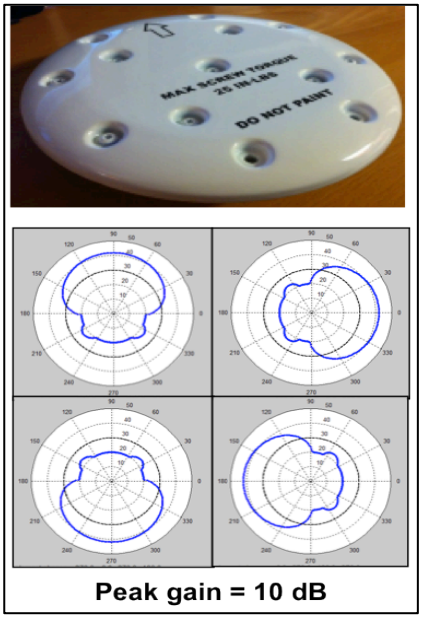

Figure 2-2. TCAS antenna and azimuth patterns.

2.2 SSPAR SURVEILLANCE OF MODE-S–EQUIPPED AIRCRAFT

Strategies for SSPAR interrogation and reception borrow heavily from the proven technology of TCAS. Mode-S aircraft acquisition will be accomplished by monitoring squitters received continuously from all directions. This means that All Call interrogations and the numerous All Call replies will be eliminated, resulting in a significant reduction in spectrum usage as we will quantify in Section 5. When a previously untracked Mode-S transponder signal is received, SSPAR will commence tracking with Roll Call interrogations, soliciting the aircraft's Mode C altitude and Mode A code.

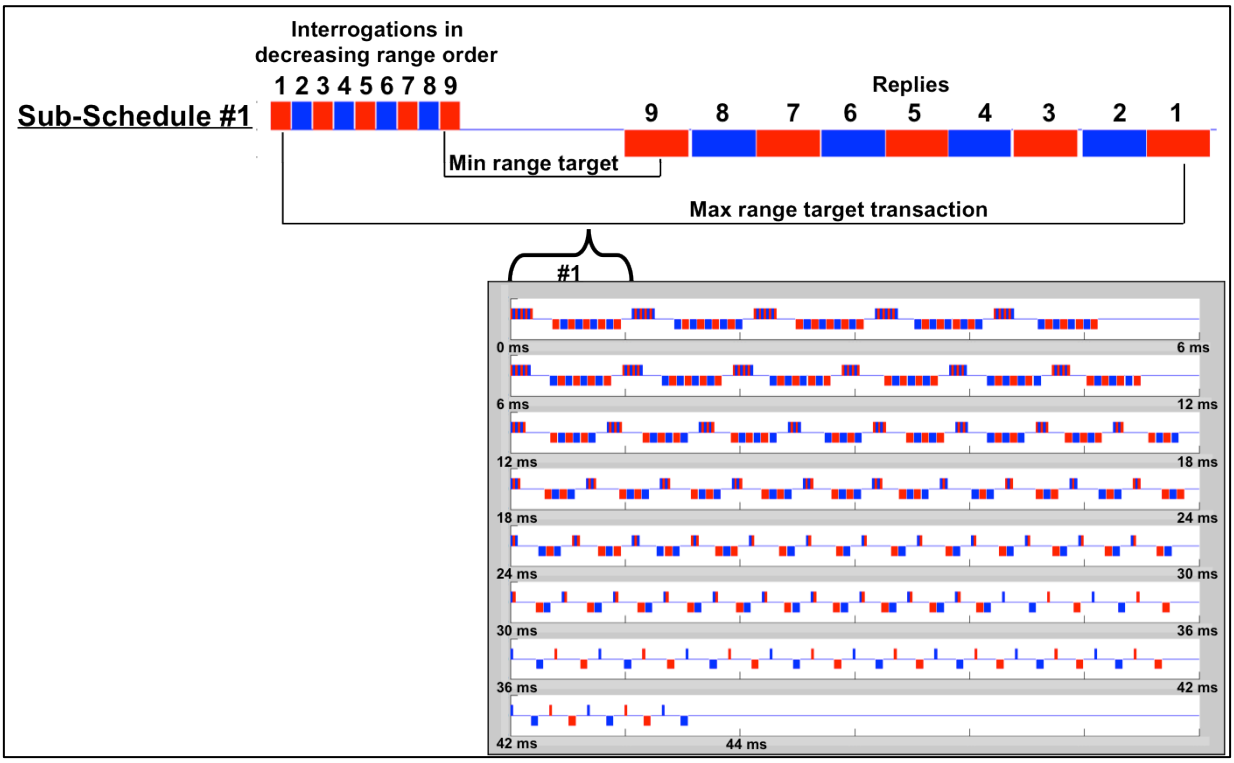

Figure 2-3. Mode-S Roll Call schedule.

Figure 2-3 depicts a simulation of an SSPAR Roll Call schedule for Mode-S aircraft. In this simulation, there are 240 targets within the 60 NM surveillance range of the sensor. The first interrogation "sub-schedule" is to the farthest target in range, followed by as many additional interrogations as will fit before the first reply is due to be received. Subsequent interrogation sub-schedules are then initiated, beginning with the farthest remaining target, until replies from all targets have been received. A key difference between Roll Call with SSPAR versus rotating SSRs is that the SSPAR interrogation beam can be electronically steered for each interrogation to the azimuth of the scheduled aircraft, as can the array receiving response. Thus surveillance updates for all tracked Mode-S aircraft within range of SSPAR can

be obtained from a single Roll Call schedule. In the simulation depicted here, SSPAR requires 76 sub-schedules and only slightly more than 40 milliseconds of elapsed time to update the positions of the 240 aircraft within range of the sensor. This extreme efficiency of SSPAR interrogation/reply for Mode-S–equipped aircraft offers significant opportunities for spectrum congestion mitigation, as well as high-update surveillance where required to support NextGen concepts of operation.

A Mode-S transponder will emit one spontaneous TCAS squitter per second, two ADS-B position squitters per second, and two ADS-B velocity squitters per second. It also replies to SSR All Calls, SSR Roll Calls, and TCAS Roll Calls. If GPS is out, or if an aircraft is not able to determine its position, the transponder will still emit the TCAS squitter and be interrogated by TCAS. In dense airspace, the numerous TCAS aircraft will elicit several replies per second per transponder. All of these above mentioned replies are candidates to be used by SSPAR to estimate the azimuth of the target. This will allow SSPAR to make azimuth measurements once per second even if the probability of getting an accurate azimuth from a single reply is less than one due to interference by other Mode-S or ATCRBS replies. In sparse airspace there will be fewer replies elicited by TCAS, but also a higher probability of getting an accurate azimuth on a given reply. Therefore, it is possible that SSPAR will usually only need to interrogate once to obtain the range of a target. The accurate measurement of range may be more likely than measurement of azimuth, because fewer non-interfered-with pulses are required to measure range. For all these reasons, SSPAR will probably not have to re-interrogate targets very often. Thus, SSPAR can provide surveillance on Mode-S targets with minimal False-Reply-Uncorrelated-In-Time (FRUIT) generation and transponder occupancy.

2.3 SSPAR SURVEILLANCE OF ATCRBS–EQUIPPED AIRCRAFT

SSPAR will accomplish ATCRBS aircraft surveillance via directional interrogation, and reception of the resulting transponder replies. As with current SSRs, SSPAR will transmit an SLS pulse to eliminate replies from aircraft outside of its interrogation beam.

Figure 2-4 illustrates a key challenge for ATCRBS surveillance referred to as synchronous garble. This occurs when multiple aircraft are separated in range by less than about 1.7 NM, which corresponds to the duration of an ATCRBS reply. The overlapped replies result in decoding errors, which may not be resolved on subsequent re-interrogations as the overlap, will persist. As an example, if the density of aircraft is 0.1 aircraft per square mile (a value typical of high-density airspace in the U.S. today) and the aircraft of interest is at a range of 20 NM, then for an omnidirectional interrogation, there would be approximately 40 additional ATCRBS replies that overlap the reply of interest. This number would increase linearly with the range from the sensor to the target of interest.

SSPAR will mitigate synchronous garble using a combination of directional interrogation, Whisper-Shout interrogation and digital array processing. The SSPAR antenna array can generate an azimuth beamwidth as small as 4^{o}, corresponding to a "garble improvement factor" of 90. However, spectrum usage and interrogation time could be reduced if a broader interrogation beam were used.

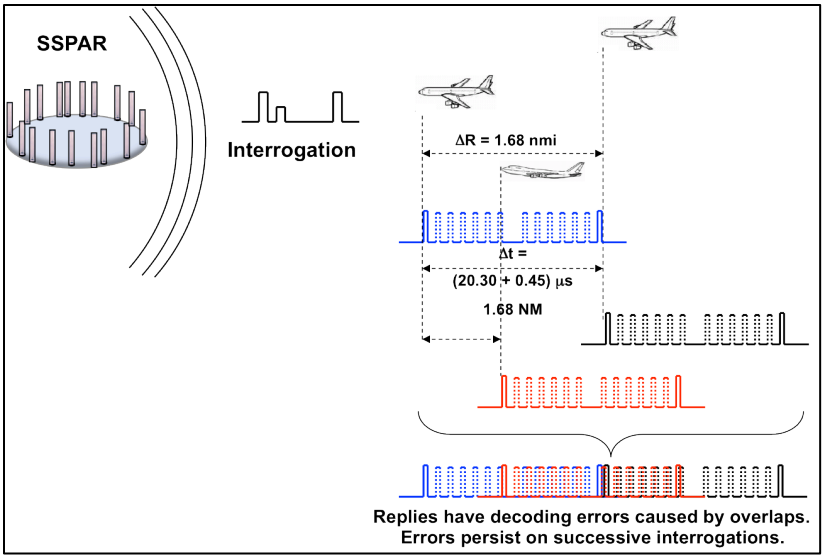

Figure 2-4. Illustration of synchronous garble.

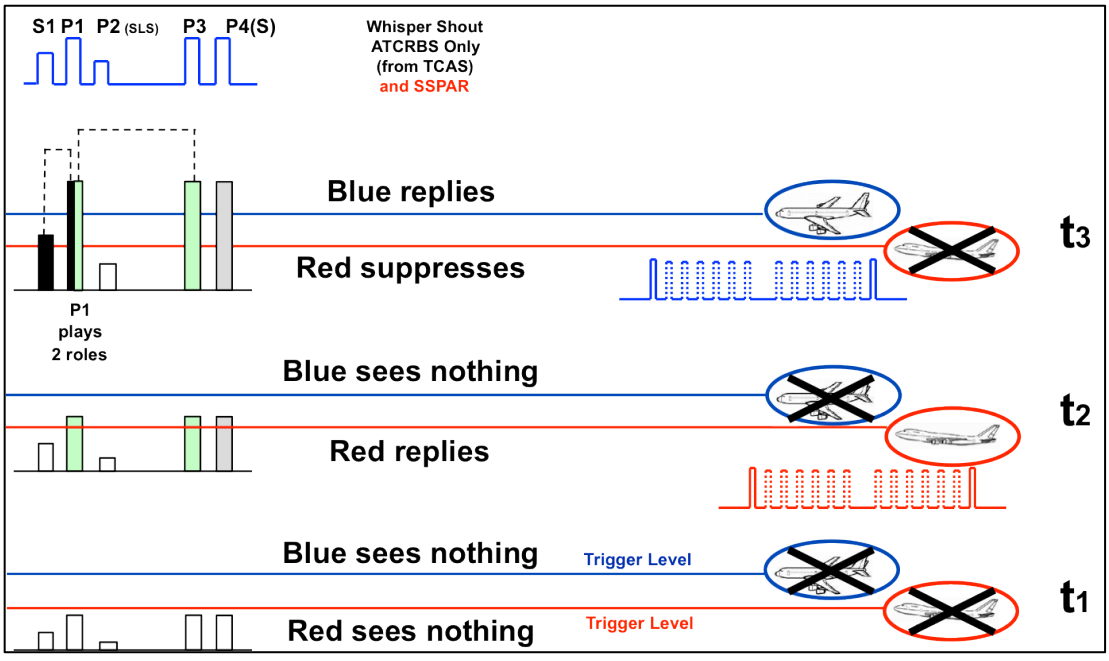

Figure 2-5. Whisper Shout interrogation for partitioning replies from closely spaced aircraft.

Whisper Shout consists of a sequence of interrogations, beginning at a low power and increasing to the final full power. The objective is to partition the replies so that only a small subset is received during any one reception period. Figure 2-5 illustrates the application of Whisper Shout to the partitioning of replies from two aircraft that are close in range. Note the addition of the suppression pulse "S1" two microseconds prior to the first pulse of the standard ATCRBS interrogation. This suppresses transponders that have already replied to an interrogation earlier in the sequence.

Finally, the adaptive array processing techniques described later in this report will also allow for decoding of overlapping replies from aircraft if they are sufficiently separated in angle, and if the number of overlapping replies is substantially less than the number of array elements (say 10 or less).

In summary, we are confident that a combination of these techniques will be effective in mitigating ATCRBS synchronous garble. Details involving the tradeoffs between interrogation beamwidth, length of the Whisper Shout interrogation sequence, and the performance of adaptive array processing techniques will be worked out through future analysis and data collection.

3. ARRAY DESIGN AND PERFORMANCE MODELING

The SSPAR array will consist of omnidirectional (in azimuth) antennae, each with an independent transmitter and receiver. For interrogation, signals transmitted by the antennae will be properly phased to steer the interrogation beam in the desired direction. The receiver output from each antenna will be separately digitized, allowing for the synthesis of "beamformers" optimized for each potential signal of interest arriving at the array. Adaptive processing increases detection and copy performance by digitally nulling interference and preserving gain to the extent possible on the signal of interest. An array with N elements can null at most N-1 sidelobe interferers.

Lincoln Laboratory has demonstrated adaptive, sparse array processing capability similar to that which will be required for SSPAR in numerous defense and intelligence applications. Beam-split (the ratio of signal direction estimate standard deviation to the physical beamwidth of the array) approaching the 70:1 goal for SSPAR have been demonstrated using appropriate array calibration approaches, even on moving platforms. For SSPAR, ADS-B–equipped aircraft of opportunity can be used to continuously calibrate the array, supporting the ability to attain very high beam-split ratios. We expect that the array should only require recalibration on time frames measured in months, or whenever new construction occurs in the vicinity of the array that changes the propagation environment. Thus the system should be robust to GPS outages lasting a number of days.

3.1 ARRAY DESIGN AND LINK BUDGET

Figure 3-1 depicts a commercially available antenna – dB Systems DME 540 – that would be suitable for the SSPAR array. The antenna consists of vertically stacked dipole elements, phased so as to produce an approximately cosecant-squared elevation pattern with a sharp cutoff below 0^o to minimize multipath. Subsequent analysis will be based on this antenna's parameters although there are likely other commercial offerings that would perform well.

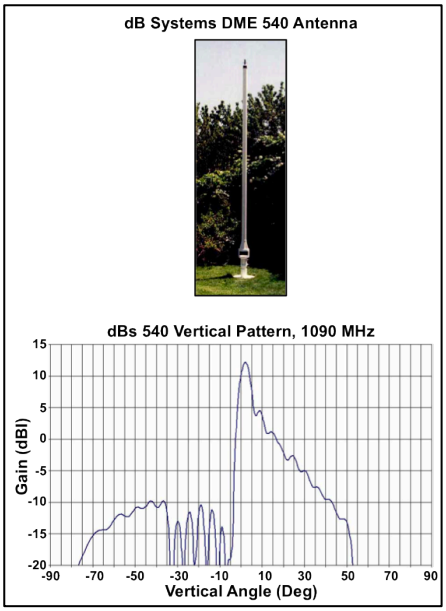

Figure 3-1. Commercially available antenna suitable for SSPAR array.

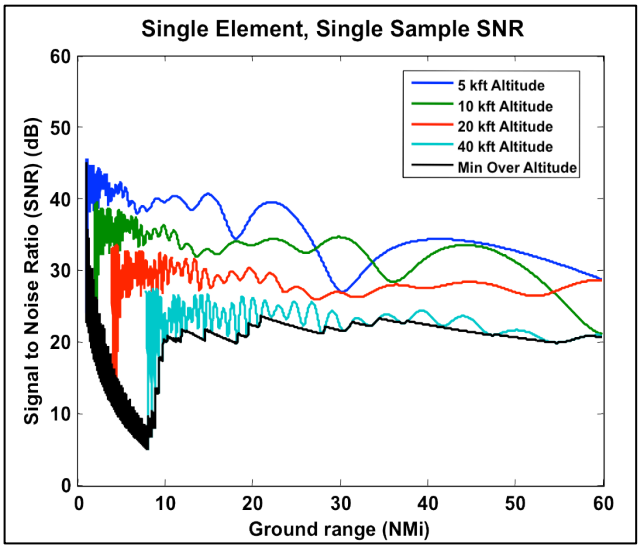

Figure 3-2. Downlink single-sample SNR as a function of range.

Figure 3-2 shows the downlink single-sample, signal-to-noise ratio (SNR) as a function of range, assuming a 125 Watt aircraft transponder at the indicated altitudes. The multipath fade for targets at short range is an artifact of the conducting, flat-earth model used for this analysis. Any actual fade could be mitigated through tuning of the antenna's elevation response. Overall, the plot indicates that SNR greater than 20 dB will be attained at all ranges and transponder altitudes. SSPAR performance will be limited not by SNR but by co-channel interference from other SSRs and transponders.

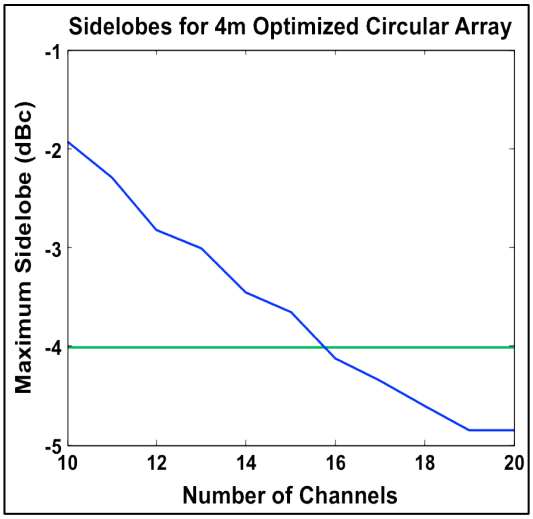

Figure 3-3. Maximum SSPAR array sidelobe level as a function of number of antenna channels.

As a function of the number of antenna elements, Figure 3-3 shows the maximum array sidelobe level for a 4 m diameter, sparse, circular array designed using numerical optimization approaches to minimize sidelobes. Lincoln Laboratory's prior experience with direction finding arrays has indicated that desired SSPAR performance can be realized if maximum array sidelobes are maintained at least 4 dB below the peak array response when steered in any direction. This level is reached for an array of 16 or greater antenna elements. For subsequent analysis, we will model the SSPAR as consisting of 17 elements, configured as shown in Figure 3-4. An example response pattern is shown, emphasizing that the sidelobes are significantly higher than is the case with a conventional radar antenna.

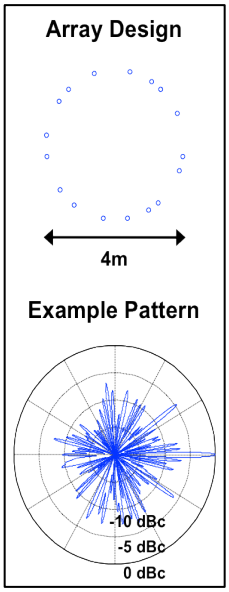

Figure 3-4. Candidate 17-channel SSPAR array and example antenna pattern.

Given this number of antenna elements, the transmit power per channel requirement can be determined. Figure 3-5 plots the output power required to trigger a transponder with a worst-case –69 dBm trigger level as a function of transponder range and altitude. Neglecting the multipath fade at short range (again an artifact of our simplistic, conducting, flat-earth model), the figure indicates that transmit power of 20 W per element would be adequate to satisfy the uplink budget. However, the sparse SSPAR array has relatively high sidelobes so that interrogations will have significant energy in many directions, not just the intended direction. To eliminate unwanted transponder replies, SSPAR will transmit an SLS pulse, using an "omni" beam synthesized by appropriately weighting transmissions from all 17-array channels. This beam will have a notch in the main transmit direction, which is required to provide the necessary 9 dB margin between the pulses transmitted through the main beam and the SLS pulse. Given the SSPAR array configuration, we have successfully synthesized the omni beam, and have found that it requires five times the transmit power of the directional beams, bringing the SSPAR transmit power requirement per channel up to 100 Watts. Note that that the power amplifiers must be in their linear operating region up to 100 Watts to assure proper synthesis of the omni pattern. As shown in Section 4, this requirement is readily achieved with commercially available parts.

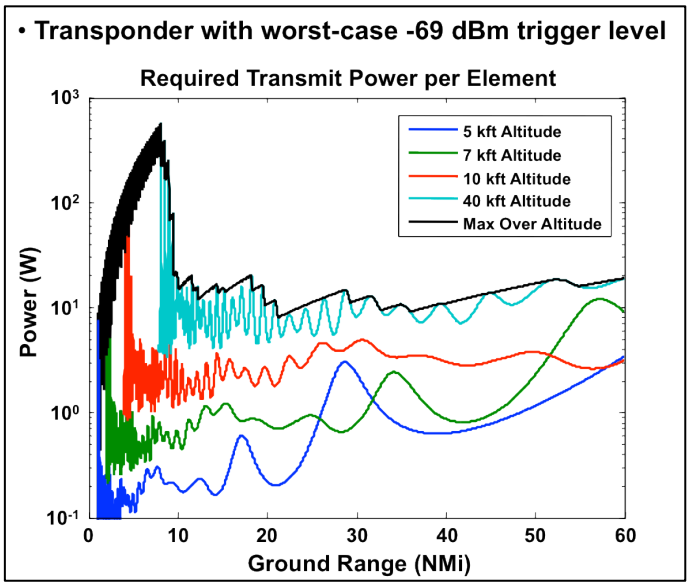

Figure 3-5. SSPAR array output power required to trigger –69 dBm MTL transponder.

Given the array design and the sensitivity of each channel we can predict a lower bound for azimuth estimate accuracy in the absence of interference. The result is plotted in Figure 3-6 as a function of SNR per element. Recall that we expect to achieve 20 dB or better SNR per element per sample. So an estimate using a single sample will have 20 dB SNR, yielding a bound of about 0.5 milliradians. If instead we use four time samples to estimate the azimuth, we gain 6 dB of SNR and the bound is approximately 0.3 milliradians. Thus in a noise-only environment, SSPAR azimuth accuracy would substantially exceed our 1 milliradian goal, assuming that the array can be very well calibrated using ADS-B targets of opportunity. Realistically, however, the presence of co-channel interference is likely to result in accuracy that is poorer than these bounds. The following subsection assesses the impact of this interference.

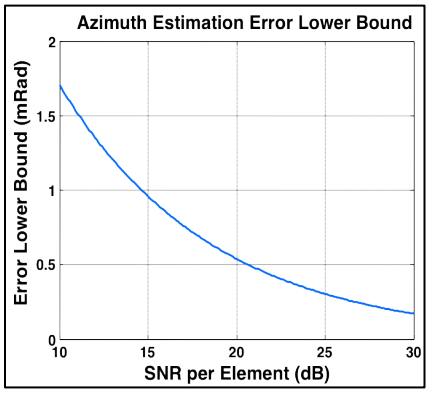

Figure 3-6. Lower bound for SSPAR azimuth estimate accuracy in the absence of co-channel interference.

3.2 IMPACTS OF INTERFERENCE ON PERFORMANCE

The analysis presented in this section uses a model for 1090 MHz interference representative of high-density airspace in 2035 (MIT Lincoln Laboratory, 2013). The left plot in Figure 3-7 presents the cumulative FRUIT rate for both ATCRBS and Mode-S transponders. For example, roughly 30,000 ATCRBS FRUIT per second are expected to be seen at SNR of 20 dB or less. We use this model to generate example FRUIT time series, assuming the azimuthal distribution of FRUIT sources is uniform, and the timing of the FRUIT follows Poisson statistics. The right plot presents the signal in a single antenna of the simulated system for one such simulation run. The time series is so dense because of the omnidirectional azimuth patterns of each element. Many such randomized time series models were generated and their statistics analyzed to better understand the FRUIT environment in which SSPAR must operate.

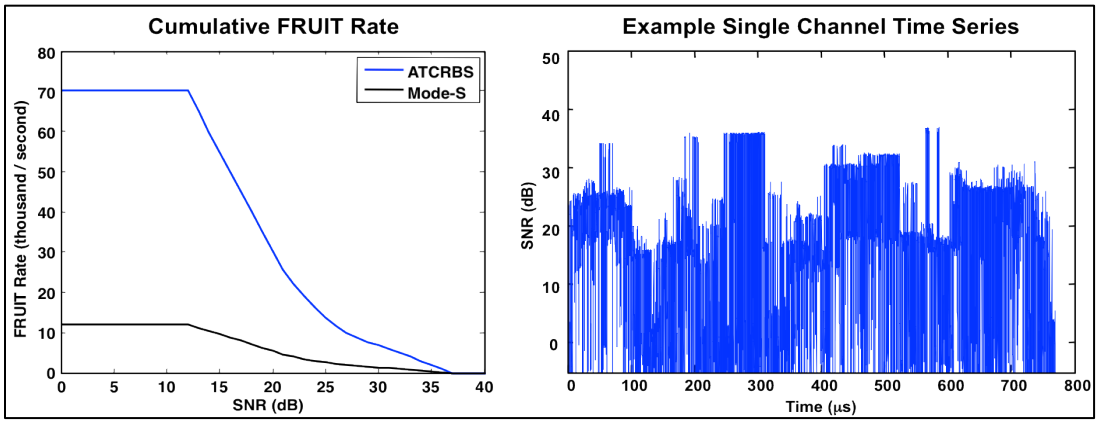

Figure 3-7. Modeled, cumulative FRUIT rate for ATCRBS and Mode-S transponders and a consistent, SSPAR single-channel time series.

One way to think about the FRUIT is to consider the number of FRUIT that will overlap a given signal of interest. In the upper right panel of Figure 3-8, an ATCRBS signal is shown, along with three notional overlapping FRUIT. If we were to use a single adaptive beamformer to detect all of the bits in this signal, then we must null all three FRUIT signals. We are particularly interested in understanding the probability that there are at least M FRUIT overlapping a given signal of interest. The plot on the left side of the figure presents this probability for each of the three transponder reply types of interest. For example, the plot indicates that if we are interested in detecting an ATCRBS reply, then with probability 0.1 there will be at least eight overlapping signals, and at least 11 overlapping signals with probability of 0.01. With 17 channels, we therefore will usually be able to use a single beamformer to detect and copy an entire ATCRBS reply. However, for the long format Mode-S signal, approximately 20% of the time there will be more than the maximum 16 interferers that can be nulled by the array. The table in the lower right displays the 0.01 overlap probabilities for our three transponder reply types.

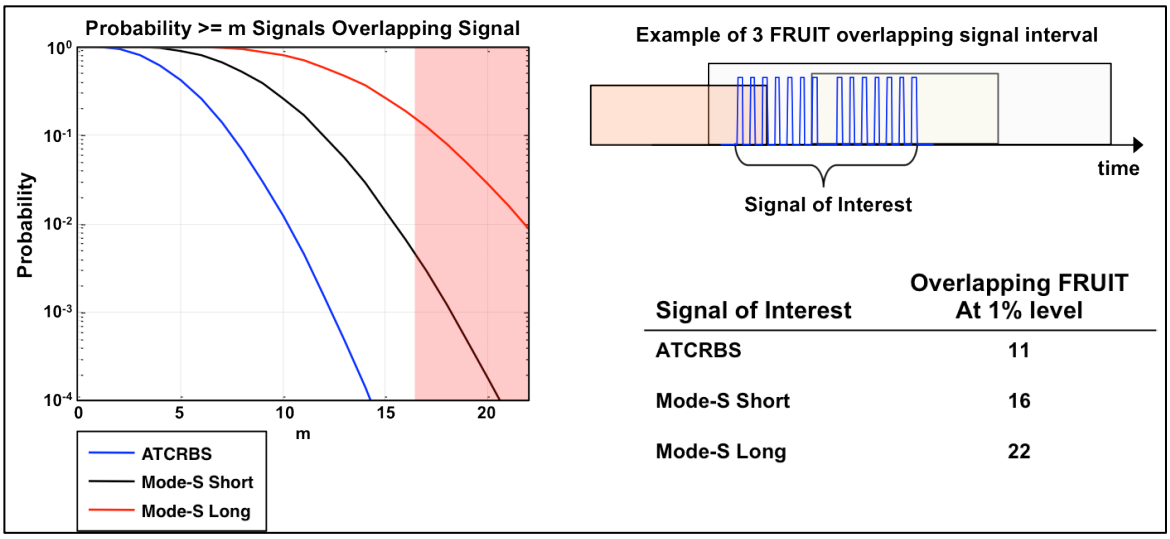

Figure 3-8. Signal overlap probability.

If we have so much interference for a given signal of interest that we cannot use a single beamformer for the entire signal, then we can consider using a separate adaptive beamformer for each pulse (bit) of each signal. Referring to the schematic in the upper right of Figure 3-9, the worst pulse only has two overlapping FRUIT. The probability that there are is least M overlapping signals in the worst pulse (bit) is plotted in Figure 3-9 for each of the three transponder replies, using Monte Carlo simulations consistent with the FRUIT model presented above. We see that even the Mode-S long (extended format) signals will have eight interferers or more only with probability 0.01. We will therefore carry eight interferers as our design point for the remaining analysis.

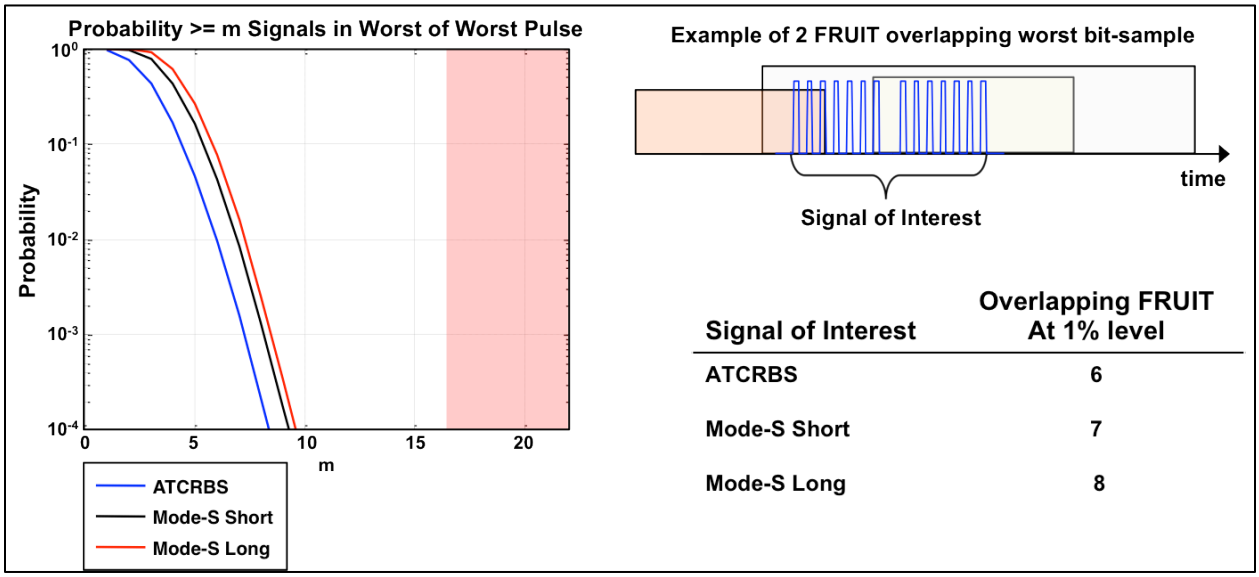

Figure 3-9. Sample overlap probability.

In order to understand the impact of nulling a number of interference sources, we performed separate Monte Carlo simulations with strong (very high SNR) interference sources coming from uniformly random azimuth angles. For the calculation, we use the 20 dB SNR per element per sample that we found in the link budget. Including the 12 dB gain realized from the 17-channel array, the resulting SNR would be 32 dB. The presence of interference requires adaptive nulling which eliminates the interference but results in less than the full 12 dB of array gain. After the processing is complete we have some amount of signal to interference plus noise (SINR) remaining.

Figure 3-10 presents the cumulative probability of SSPAR obtaining a given SINR for one to ten interference sources. For example, our design point of eight interference sources results in a probability of 0.99 of having at least 26 dB SINR. This is a high SINR for detection purposes so we expect the 17-channel system to function well, even in a dense FRUIT environment.

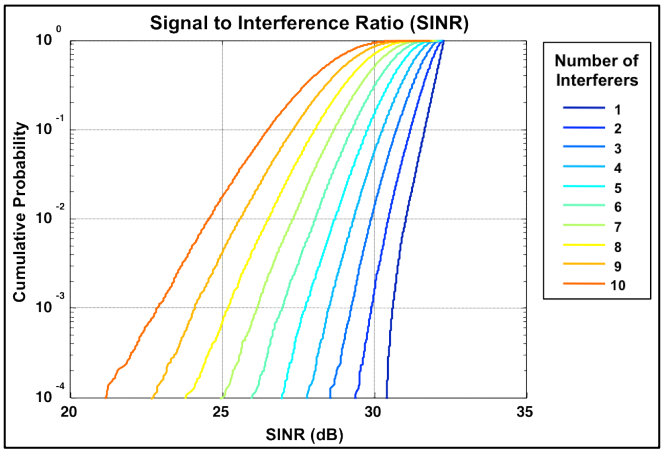

Figure 3-10. Cumulative probability for SSPAR array output signal to interference plus noise ratio.

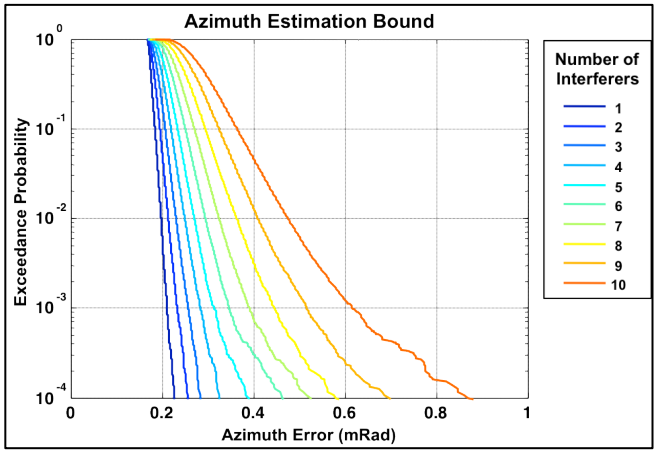

Figure 3-11. Exceedance probability for SSPAR azimuth error.

The process of nulling interferers may also reduce the azimuth estimate accuracy for the reply of interest. We used the Monte Carlo simulations to determine azimuth estimate accuracy as a function of the number of interferers, assuming perfect array calibration. Here we assume that we are using 10 time samples (the number we expect to get for 2–3 ATCRBS pulses or a Mode-S bit) in our estimate. Figure 3-11 plots the exceedance probability for azimuth estimate accuracy lower bound for the different number of strong interference sources. For eight interference sources, the probability is 0.99 that azimuth estimate accuracy lower bound will be better than 0.4 milliradians.

This error analysis assumes that the azimuth estimate was not getting lost on a sidelobe of the antenna. However, given the high sidelobes of the SSPAR array there is a possibility that a given estimate will end up on a sidelobe instead of in the mainlobe. In order to estimate the likelihood of this happening, we used our FRUIT model-based Monte Carlo simulation to quantify how poor the sidelobes were after nulling each example set of interference sources. The cumulative probability of the peak to sidelobe ratio is presented in the left panel of Figure 3-12. For our eight interferers design point, there is a 0.99 probability that the peak sidelobe is more than 1.25 dB down from the mainlobe. The right panel is an analytic calculation of the probability that the azimuth estimate is corrupted by landing on an antenna sidelobe, plotted as a function of the peak to sidelobe ratio for several different SINR values. For the 1.25 dB peak to sidelobe ratio and the SINR values expected for SSPAR (see Figure 3-10), the probability that a sidelobe will corrupt the SSPAR azimuth estimate is negligible.

For the actual SSPAR system, array calibration errors would degrade the direction estimates relative to the analysis presented above. However, with the abundance of ADS-B calibration signals, and the fact that Lincoln Laboratory has demonstrated equivalent accuracies on other sparse adaptive arrays that had less calibration data, we infer that it is highly likely that the 1 milliradian azimuth estimate accuracy goal for SSPAR can be achieved.

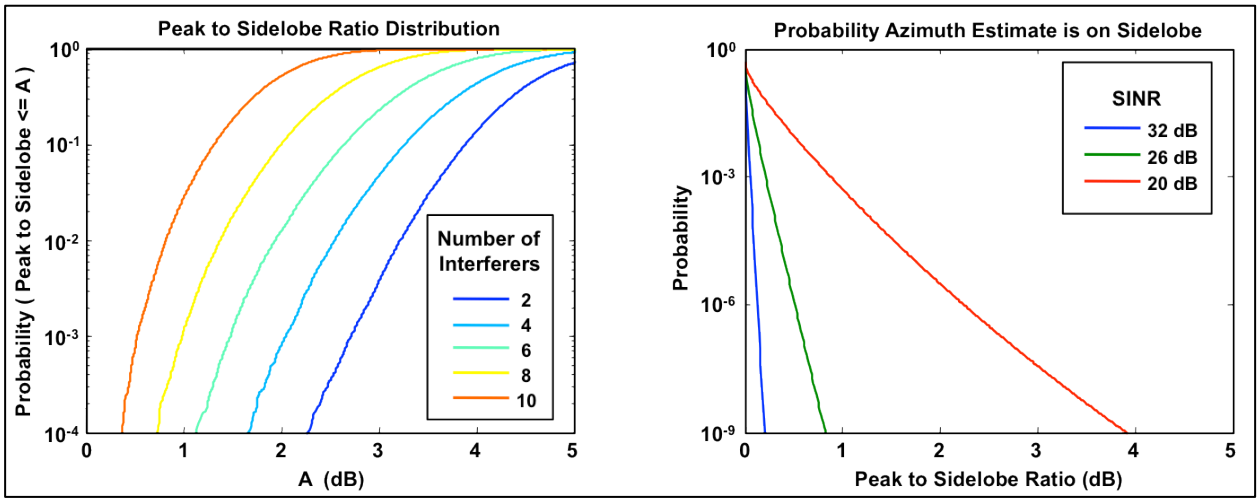

Figure 3-12. SSPAR array peak to sidelobe ratio distribution and probability that azimuth estimate is captured by a sidelobe.

3.3 PROCESSING AND SIMULATION EXAMPLE

The general processing approach we propose to use is called Adaptive Event Processing (AEP) and has been used in sparse array signal detection, copy, and direction finding for several decades (Forsythe, 1997). Figure 3-13 illustrates the approach. It is convenient to consider each time sample to be a vector of length 17, since for each time we receive signals from all 17-array channels. The technique is applied by

selecting some number of these time samples as “training data” and then to look for signals in the “test data” that are not present in the training data. In effect this is an extension of the well-known “constant false-alarm rate (CFAR)” processing technique to an array-based system. As indicated in the figure, AEP is effective for detecting pulse edges, it provides interference-nulling beamformers to use for each detected pulse and provides azimuth estimates for the signal of interest. Although many details of the application of AEP to the SSPAR processing challenge remain to be worked out, it is useful to present a preliminary simulation demonstrating its effectiveness.

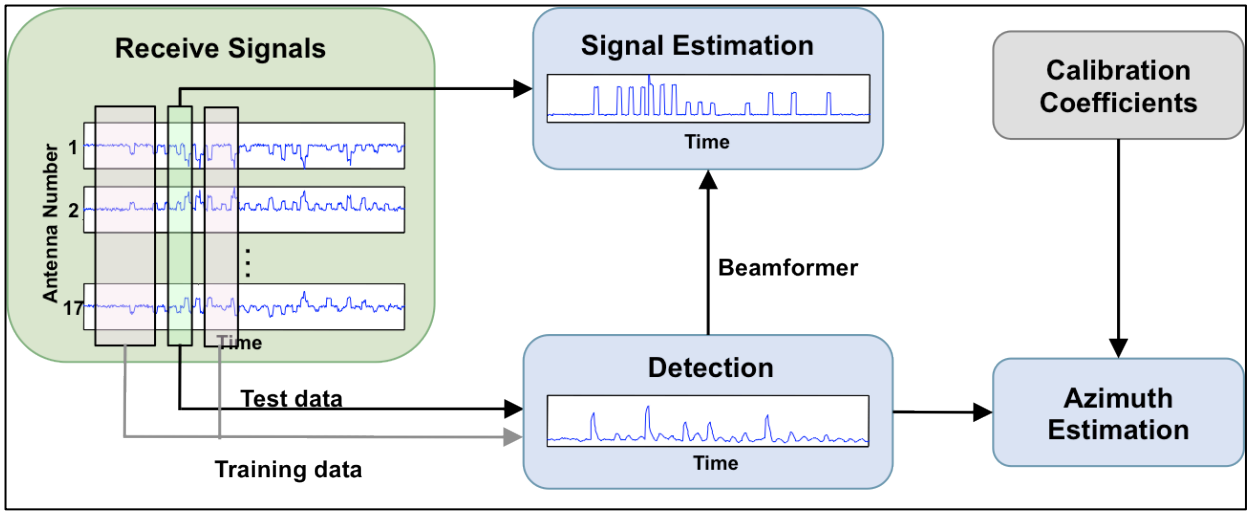

Figure 3-13. Adaptive Event Processing (AEP).

Figures 3-14 and 3-15 present a simulation of AEP processing applied to transponder replies received on an SSPAR array. The AEP framework has been used to design a detector to find the leading edge of ATCRBS signals. Recall that for ATCRBS we will usually have few enough interference signals that we can use a single beamformer for the entire signal. The detector was designed by using the gaps between the ATCRBS pulses in the training data, and testing on the leading edge of the first frame pulse. The example time series is from the FRUIT model-based simulation discussed earlier. The reply of interest is a new ATCRBS signal beginning at time 77 microseconds. The AEP detection statistic is presented in the lower panel, and a single strong peak is found that coincides with the beginning of the ATCRBS signal. Figure 3-15 shows the signal estimate formed from the array time series using the beamformer generated by AEP. Although no attempt has been made to normalize the signal amplitude estimate, it is obvious that the ATCRBS reply has been copied with high fidelity. This level of performance is typical of the simulations we have performed for ATCRBS replies to date.

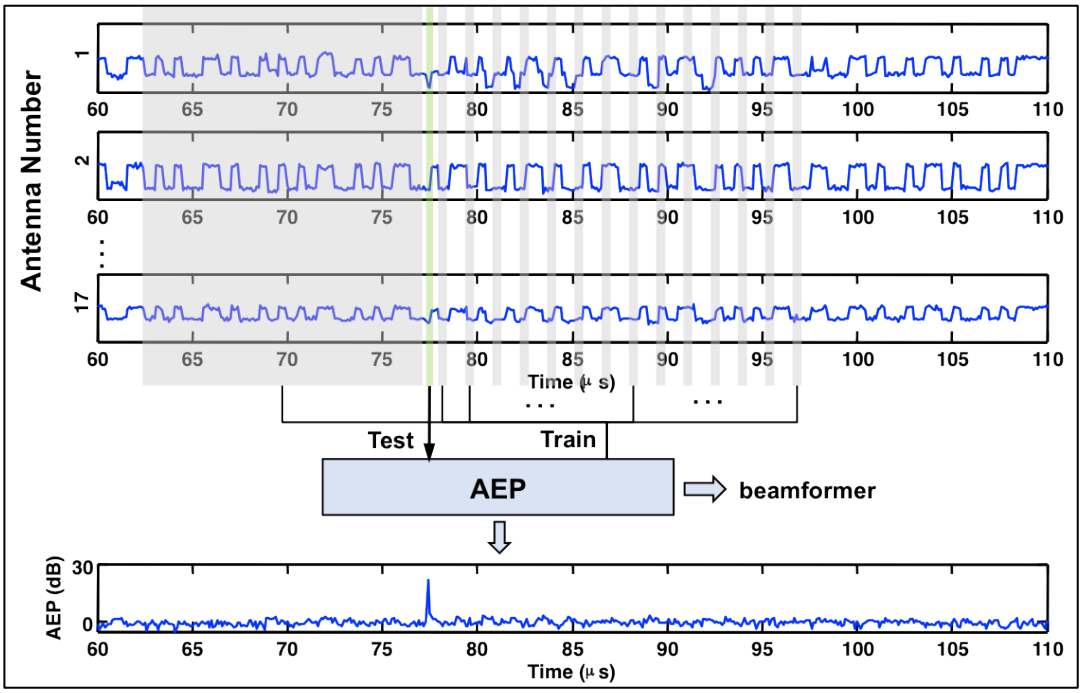

Figure 3-14. Simulated SSPAR time series and AEP leading edge detector output for ATCRBS reply starting at T = 77 us.

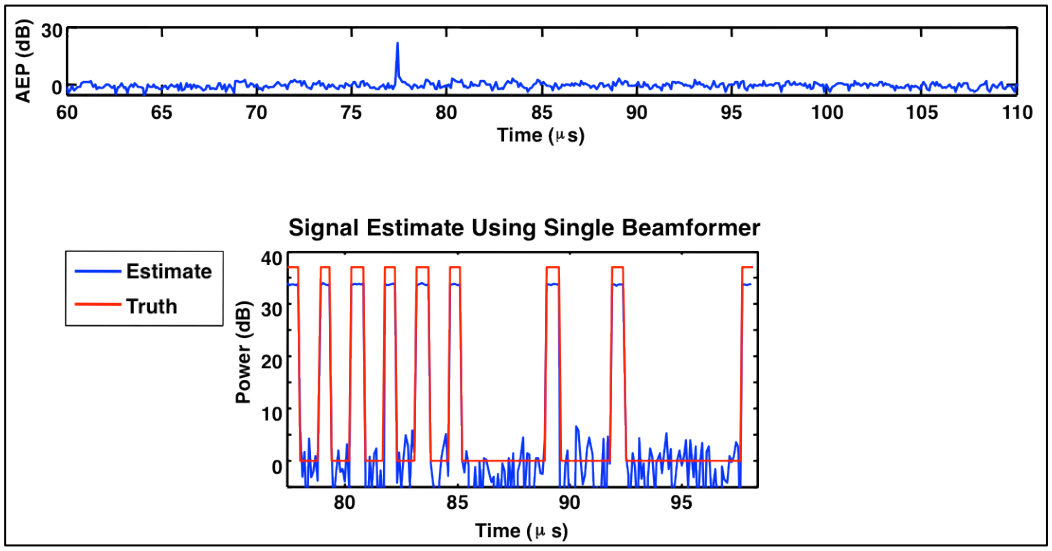

Figure 3-15. ATCRBS signal estimate.

Further work is needed to confirm the ability to detect, direction-find, and copy the longer-duration signals associated with Mode-S replies and short- and long-squitters from Mode-S transponders. As noted, this will require beamformers that adapt continuously to the interference environment over the duration of the signal of interest. While we are confident that robust algorithms can be developed, ongoing modeling, simulation, and data collection/analysis will be required to flesh out details of the processing.

This page intentionally left blank.

4. PRELIMINARY SSPAR SYSTEM CONFIGURATION AND RECURRING COST ESTIMATE

Figure 4-1 is a high-level SSPAR system diagram. Key subsystems are the radar controller, responsible for interrogation management and track maintenance, the signal, and data processor, which may exploit commercial high-capacity graphic processing units (GPU), receiver/exciters and transmit/receive (TR) modules for each of the 17 channels of the SSPAR array. The shelter electronics would be connected to the antenna elements using low-loss RG-213 cable.

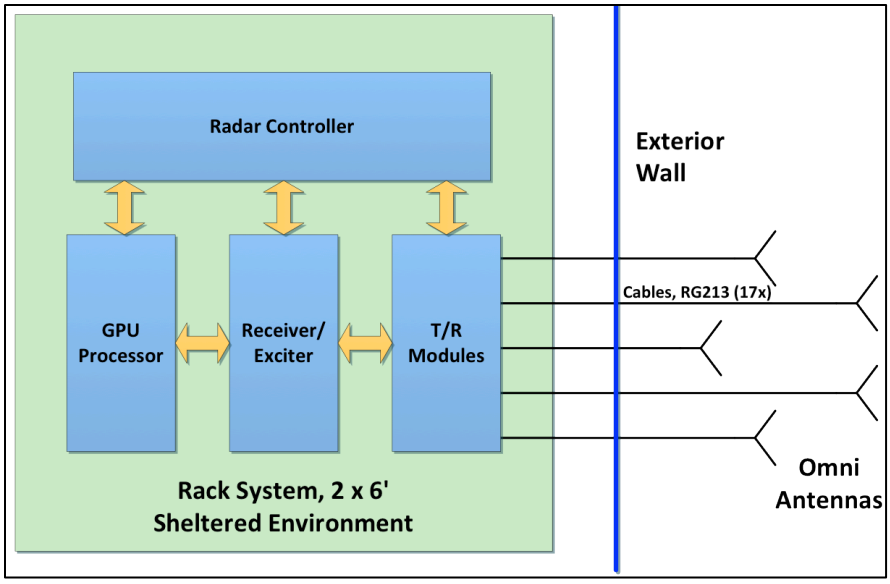

Figure 4-1. SSPAR system block diagram.

As noted previously, a candidate antenna for the SSPAR system is the dB Systems 540 described in Section 3. An alternative would be the lower cost dB Systems 5100, which has fewer dipole elements in each column and as a result, 3 dB lower antenna gain. The loss in uplink SNR can be overcome by larger TR module power amplifiers to maintain necessary power levels for transponder interrogation. The 3 dB downlink loss of SNR for transponder replies would not be expected to affect array detection, direction-finding, and copy performance as is evident from the discussion in Section 3.

Table 4-1 defines TR module requirements, based on analysis presented in the preceding section. Key requirements are transmit linear output power, small signal gain, receiver noise figure, and third order intercept. Although we have not identified commercially available integrated TR modules meeting these requirements, a custom implementation using COTS components could be readily developed.

Table 4-1

SSPAR TR Module Requirements

Mode	Parameter	Comment	Min	Max	Units
Transmit	Frequency		1020	1040	MHz
	$Power_{SAT}$		600		W
	$Power_{LIN}$	P_{SAT} – 7dB	120		W
	Modulation	Pulse, DPSK	--	--	
	Gain	Exciter Po ~ -10dBm	70		dB
	Post-PA Loss	Circ., Cable		1.5	dB
Receive	Frequency		1080	1100	MHz
	Gain		20		dB
	Noise Figure	NF		3	dB
	Input Third Order Intercept	IIP3	10		dBm
	Pre-LNA Loss	Circ., Cable, Filter		2	dB

Figure 4-2 is a block diagram of an appropriate SSPAR TR module. This has two variants that differ by the number of power amplifiers (2 or 4) corresponding to the choice of antenna discussed in the previous paragraph. Each power amplifier has 300 W saturated power capability, resulting in 600 or 1200 W output power capability. TR functionality is enabled by the use of a high power, high isolation circulator. The circulator minimizes load-pull effects on the power amplifier due to a variable antenna match and shields the low noise amplifier (LNA) from direct exposure to the transmitter power amplifier output. If needed, a TR switch can be added to the receive path, post circulator, to provide additional transmit mode protection. The bandpass filter shown in the receive path blocks LNA saturation due to out-of-band emitters.

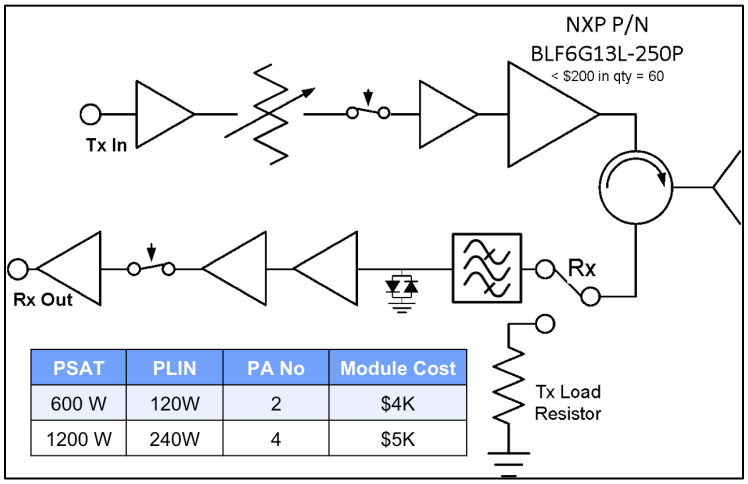

PSAT	PLIN	PA No	Module Cost
600 W	120W	2	$4K
1200 W	240W	4	$5K

Figure 4-2. SSPAR TR module block diagram.

An appropriate power amplifier for the SSPAR TR module is the NXP COTS amplifier depicted in Figure 4-3. In small quantities it sells for <$200. The picture shown at top left is of the amplifier in the matched configuration required for efficient operation. The graph shows measured gain and power-added efficiency (PAE) as a function of Power Out. This type of graph, gain versus power out, is called a compression curve.

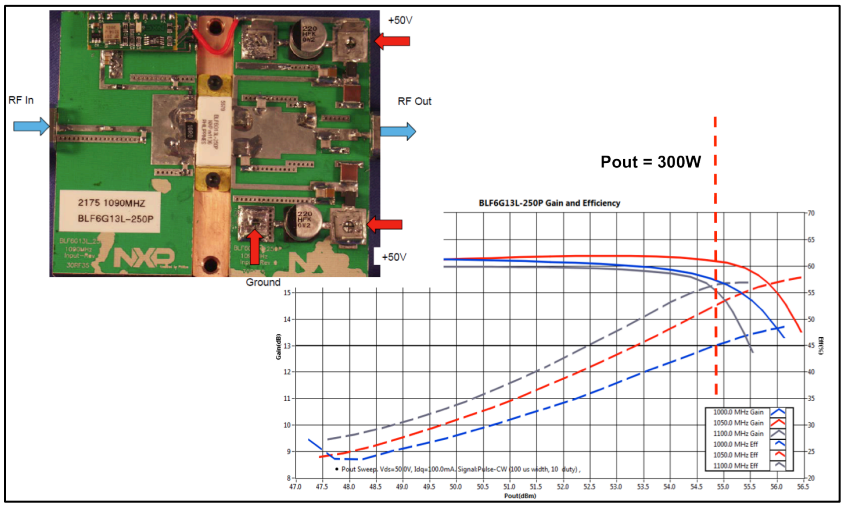

Figure 4-3. An example of a suitable COTS power amplifier for the SSPAR TR module.

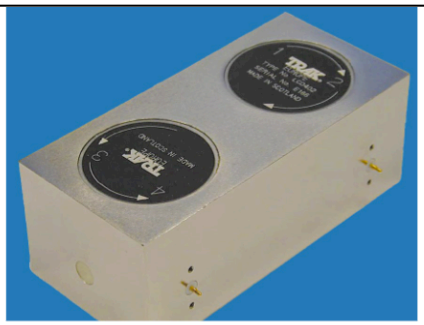

Specifications

Parameter		Specification			Unit
Frequency		1020 - 1100			MHz
		Min	Typ	Max	
Isolation	Ports 2 to 1	18	21	-	dB
	Ports 4 to 3	18	21	-	dB
	Ports 3 to 2	46	50	-	dB
	Ports 1 to 4	46	50	-	dB
Insertion Loss	Ports 1 to 2	-	0.2	0.25	dB
	Ports 3 to 4	-	0.2	0.25	dB
	Ports 3 to 2	-	0.4	.05	dB
	Ports 1 to 4	-	-	0.5	dB
Return Loss		20	25	-	dB
Forward Power		-	-	5	kW pk.
Forward Power		-	-	3.25	kW avg.
Operating Temperature		0	-	+60	°C

Figure 4-4. An example of a suitable COTS duplexer for the SSPAR TR module.

Figure 4-4 shows a dual-puck circulator or duplexer appropriate for the SSPAR TR module. This is a COTS part from Trak Europe. Its performance in the band of interest is excellent with low loss and high isolation. It also has excellent high power capability. A suitable low noise amplifier, the COTS HMC617 from Hittite is summarized in Figure 4-5. Its noise figure and third-order intercept at 1090 MHz are well suited to the SSPAR application.

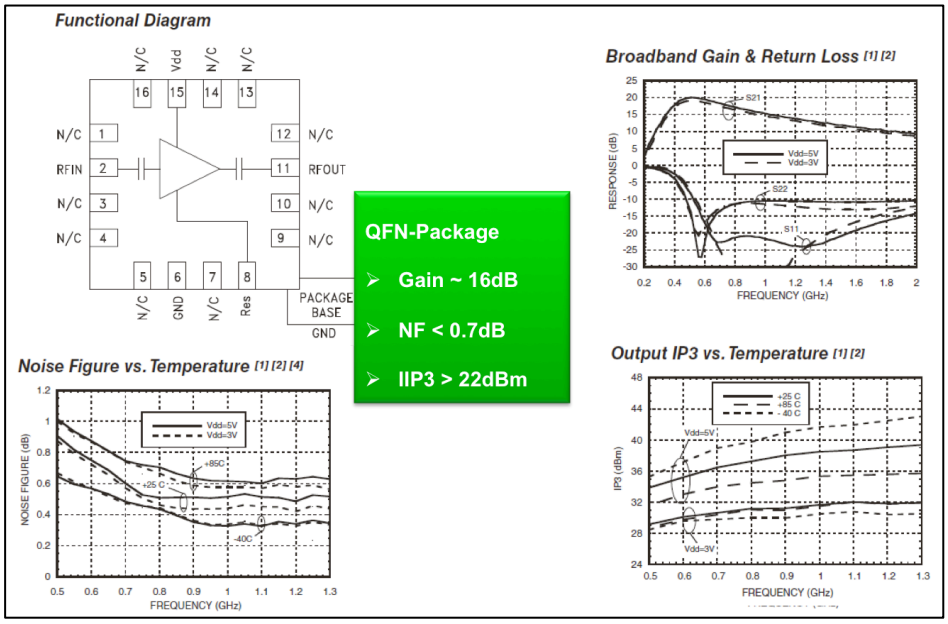

Figure 4-5. Performance parameters for a suitable COTS LNA for the SSPAR TR module.

An SSPAR COTS receiver/exciter solution is the Pentek PN52661/52671 shown in Figure 4-6. This provides quad downconverter/receivers and quad upconverter/exciters that would work well with the SSPAR concept. Fully populated digital receiver/exciter (DREX) chasses would cost approximately $130K for a 17-element SSPAR array. Pentek also provides a software suite that is used to configure the cards for the particular application and provide the control interface for the real-time radar controller.

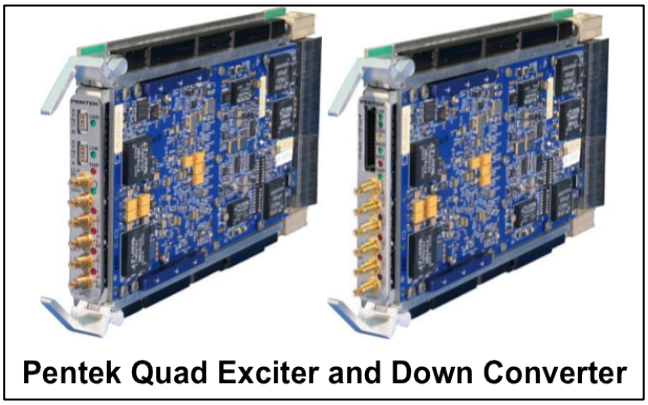

Figure 4-6. An example of a suitable COTS receiver/exciter for SSPAR.

Table 4-2 summarizes rough-order-of-magnitude pricing for the hardware needed for the SSPAR system. The cost elements considered are the antennas, the TR modules, the receiver exciter cards and chassis, and the system controller/GPU-based processor. Unit costs were taken from vendor quotes based on build quantities of 10 systems/year. Two system configurations were considered, differing by the gain of the antennae as discussed previously. With the lower gain, lower cost antennae, a loss in system SNR can be overcome by a higher power output amplifier in the TR module. In either scenario, the recurring hardware costs of the SSPAR system are low (significantly less than $500 K per system).

Table 4-2

Rough Order of Magnitude Cost Estimates for SSPAR System Components

Configuration	Cost Element	Source	Unit Cost ($K)	System Cost ($K)
17 Elements High Gain Antenna	Antenna	dBS 540	7	
	T/R Module	Custom Linear Po = 120W	4	
	Receiver/ Exciter	Pentek	9	
	Controller/ GPU Processor	COTS	3	
	Total		**23**	**390**
17 Elements Low Gain Antenna	Antenna	dBS 5100	3.5	
	T/R Module	Custom Linear Po = 240W	5	
	Receiver/ Exciter	Pentek	9	
	Controller/ GPU Processor	COTS	3	
	Total		**19.5**	**330**

In summary, SSPAR implementation carries very low risk as there is a strong competitive market in terms of price and capabilities for the components required for the system. Cell tower amplifiers at L-band are very cost effective at less than $1 per watt. Although we considered NXP, there are other very strong suppliers including Skyworks and MACOM. For the antennae, we focused on dBS but other offerings will likely provide fully acceptable performance. Finally, the Trak duplexer, a four port circulator, is a strong performer in terms of insertion loss, isolation, and power handling, and is tuned exactly to the 1030/1090 MHz bands used in secondary surveillance systems.

5. SSPAR SPECTRUM USE ANALYSIS

5.1 TRANSPONDER OCCUPANCY DUE TO 1030 MHZ UPLINK ACTIVITY

SSR and TCAS transmissions at 1030 MHz that are above a transponder's minimum trigger level (MTL) cause the transponder to either reply or "suppress." In either case, the transponder is "occupied" and unable to reply to succeeding interrogations for a period of time. The time of disablement varies according to the type of transponder and whether the transmission is intended to elicit a reply or not. The power of the interrogation or the suppression transmission determines the two-dimensional region of airspace in which transponders can hear it and thus be occupied. If the transmission is omnidirectional, then the region is a circle. If the transmission is directional, then the region is characterized by a main lobe and various sidelobes; however, the two-dimensional area of impact is the same as that of a circle whose radius is related to the power input to the antenna. It can be shown (Harman, 1977) that omnidirectional 250 W transmissions to an omnidirectional monopole receiver having a –74 dBm MTL will reach 30 NM.

Transponder occupancy is usually expressed as the percent of a second during which the transponder is occupied. Occupancy is evaluated by assessing the occupancy caused by one SSR of a particular type, and multiplying that by the number of such SSRs that the transponder can hear on average. Every uplink transmission affects an area equivalent to a circle with radius related to the power. For a given number of transmissions per second from an SSR with various power levels, the associated transponder occupancy is equivalent to a readily calculated number of transmissions at 250 W. In particular, the occupancy due to ATCRBS or All Call interrogations at a given pulse repetition frequency (PRF), experienced by a transponder within 30 NM of the SSR, is proportional to the SSR's power (divided by 250 W) times its PRF, times the occupancy time of a typical transmission (Equation 5.1). By convention, the occupancy time of one interrogation or suppression is taken to be 35 us.

$$\text{Occupancy} = 35 \times 10^{-6} * P_{xmt} * \text{PRF} / 250 \qquad (5.1)$$

As an example, if an ATCRBS Sliding Window SSR's power is 250 W, and the PRF is 286 (i.e., a pulse repetition interval (PRI) of 3.5 ms), then the occupancy due to the SSR is 1%. In the Northeast, a transponder would be within 30 NM of perhaps 3 to 7 SSRs resulting in as much as 7% occupancy.

Monopulse SSR (MSSR) or Mode-S would use a similar power, but lower PRF due to the use of monopulse for azimuth measurement. The occupancy due to Mode-S Roll Calls is less than that due to the All Calls: for example, two Roll Calls every 4.6 seconds to each of 150 Mode-S transponders would amount to about 65 transmissions per second, less than the All Call PRF. (One Roll Call elicits the Mode A code and the Mode C altitude.)

Table 5-1

Relevant Interrogation Parameters and Associated Transponder Occupancy for Current Secondary Radars and SSPAR

- **The occupancy of a narrow rotating beam SSR**

$$Occupancy = \tau \sum_{i=1}^{I} \frac{P_i}{250} = 35*10^{-6} \frac{P_{xmt} * PRF}{250}$$

And where:

T_{scan} = Scan time

RL = Run Length (interrogations/replies per beam dwell)

NB = Number of Beams = 360° / Beamwidth

PRF = Pulse Repetition Frequency (Interrogatoin per second)

$T_{scan} * PRF = NB * RL$

	ATCRBS Mode			
	ATCRBS Sliding Window	**Mode S**	**SSPAR 5 degree beam**	**SSPAR Big Bang**
BeamWidth	3.6	3.6	5.0	Omni
NB	100	100	72	1
RL	16	6	6	4
Tscan	4.6	4.6	4.6	4.6
PRF	348	130	94	0.432
Power transmit	350	350	370	4000
Pwr*PRF/250	487	182	139	14
Occupancy	0.017	0.006	0.005	0.0005
Retries	0	0	0	TBD
Total	0.017	0.006	0.005	0.00049 + TBD

SSPAR with single omni ATCRBS interrogation would cause very little transponder occupancy due to ATCRBS

Table 5-1 summarizes relevant interrogation parameters and associated occupancy time for current SSRs and SSPAR. The first two columns treat ATCRBS and Mode-S. Note that PRF can be determined by the product of beam dwells per second (NB) and interrogations per dwell or run length (RL). As noted above, the sliding window ATCRBS interrogation scheme requires a significantly higher PRF than is used for Mode-S, resulting in correspondingly higher occupancy.

The third column of Table 5-1 treats SSPAR, which would interrogate ATCRBS transponders with the "ATCRBS Only" interrogation (assuming the Terra-fix has been removed). If the SSPAR used a 5 degree wide interrogation beam, it would need about the same power as a sliding-window ATCRBS. SSPAR's use of monopulse-like processing would allow a PRF of less than one third of the ATCRBS. Thus an SSPAR interrogating ATCRBS transponders at the rate of today's surveillance radars (once per

4.6 seconds) would result in transponder occupancy about the same as a Mode-S sensor and about 1/3 of that produced by an ATCRBS sensor.

Note, however, that two unique capabilities of SSPAR could reduce transponder occupancy to values significantly less than that for a Mode-S sensor. As outlined in Section 2, SSPAR could interrogate with a spoiled transmit beam and rely on the adaptive array processing to separate overlapping transponder replies from different directions. This would reduce the average PRF since fewer beam directions would need to be interrogated for a given surveillance update period. The fourth column of Table 5-1 shows the extreme case where we assume that an omnidirectional transmit beam can be used. If this were feasible, SSPAR's ATCRBS-mode impact on transponder occupancy would be as much as a factor of 10 less than Mode-S sensor impact (depending on whether significant numbers of re-interrogations were necessary).

A second SSPAR occupancy reduction approach would be to separate SSPAR's "track" and "search" functions. The electronically steerable beam could be used to routinely interrogate only in the direction of tracked ATCRBS targets (e.g., every 4.6 seconds), thus reducing the average PRF in the frequent circumstance where not all beams intersect ATCRBS aircraft. A more slowly updating "search" scan could be executed to identify aircraft that have just taken off, or have entered the search volume at its maximum range perimeter. The occupancy reduction achieved using this strategy would depend on the density of air traffic and details of the interrogation approach for the track and search functions.

A Mode-S SSR causes occupancy during the transmissions of All Calls to Mode-S transponders, which are emitted with full power at a PRF of about 100 HZ. Consistent with Table 5-1, the Mode-S All Calls would produce additional spectrum occupancy of about 1% for transponders within range of the sensor. SSPAR would not cause any occupancy for Mode-S acquisition, because this is done passively by listening to squitters instead of interrogating for All Call replies. SSPAR's occupancy due to Roll Calls would be about the same as the Mode-S SSR, since each would need to interrogate each target twice per 4.6 second scan.

In summary, in ATCRBS-mode, transponder occupancy with SSPAR would be no greater than current Mode-S sensors, and could be substantially less depending on the efficacy of the two occupancy reduction approaches described above. SSPAR would additionally produce a large occupancy saving for Mode-S transponders in that All Call acquisition would not be required.

5.2 FALSE REPLIES UNCORRELATED IN TIME (FRUIT)

The surveillance community performed many analyses of activity on the 1090 MHz downlink channel during the development of the Mode-S system, TCAS, and ADS-B. One such analysis has been developed by MITRE (Jones, 2008), and recently augmented by Lincoln Laboratory ("Investigation of Spectrum Impact," 2013) to support FAA's 1090 MHz Congestion Mitigation Program. The analysis has parameters to describe the SSR environment and aircraft environment. Here we use this analysis framework to investigate six scenarios:

1. Year 2011 aircraft density and SSRs (where the Mode-S SSRs are Terra-fixed);

2. Same as 1, but with the Terra-fix removed;

3. Same as 1, but with Terra-fixed SSPARs replacing terminal ATCRBS and Mode-S SSRs;

4. Same as 3 but with the Terra-fix removed;

5. Year 2035 aircraft density and 2011 SSRs (with Terra-fix removed); and

6. Same as 5, with SSPAR replacing terminal ATCRBS and Mode-S SSRs.

The FRUIT rates for each scenario are determined by type of FRUIT, which are:

1. Mode-S, due to: All Call, Roll Call, TCAS Roll Call, Squitter, 1090 MHz Extended Squitter; and

2. ATCRBS, due to: Sliding Window, Mode-S with Terra-fix, Mode-S without Terra-fix, TCAS Whisper Shout, uplink field (UF) Conversions.

UF Conversions are a phenomena discovered by the FAA Technical Center, in which transponders that fail to detect the suppression pulse pair that precedes a Mode-S interrogation might interpret the rest of the interrogation as containing a P1 P3 ATCRBS interrogation pair.

Figure 5-1 summarizes modeled Mode-S and ATCRBS fruit rates for each of the six scenarios. In the upper part of the figure, modeled aircraft equipage is summarized both as percentages, and by count. For each SSR scenario the FRUIT rates are shown in the stacked bar charts, categorized by color as explained on the right. Let us focus on the 2035 scenarios and compare the current SSRs to SSPAR, both with Terra-fix removed. We see that SSPAR produces less Mode-S FRUIT, because the All Calls (in brown) are not used by SSPAR. We also see that the SSPAR scenario results in much less ATCRBS FRUIT, because SSPAR is assumed to have replaced ATCRBS and MSSRs. These legacy radars provide surveillance for Mode-S targets by eliciting ATCRBS replies whereas SSPAR will use Mode-S Roll Calls. Note that the modeled FRUIT reductions using SSPAR will be quite beneficial in offsetting the large increase in ADS-B 1090ES (shown in light blue) that will occur between 2011 and 2035.

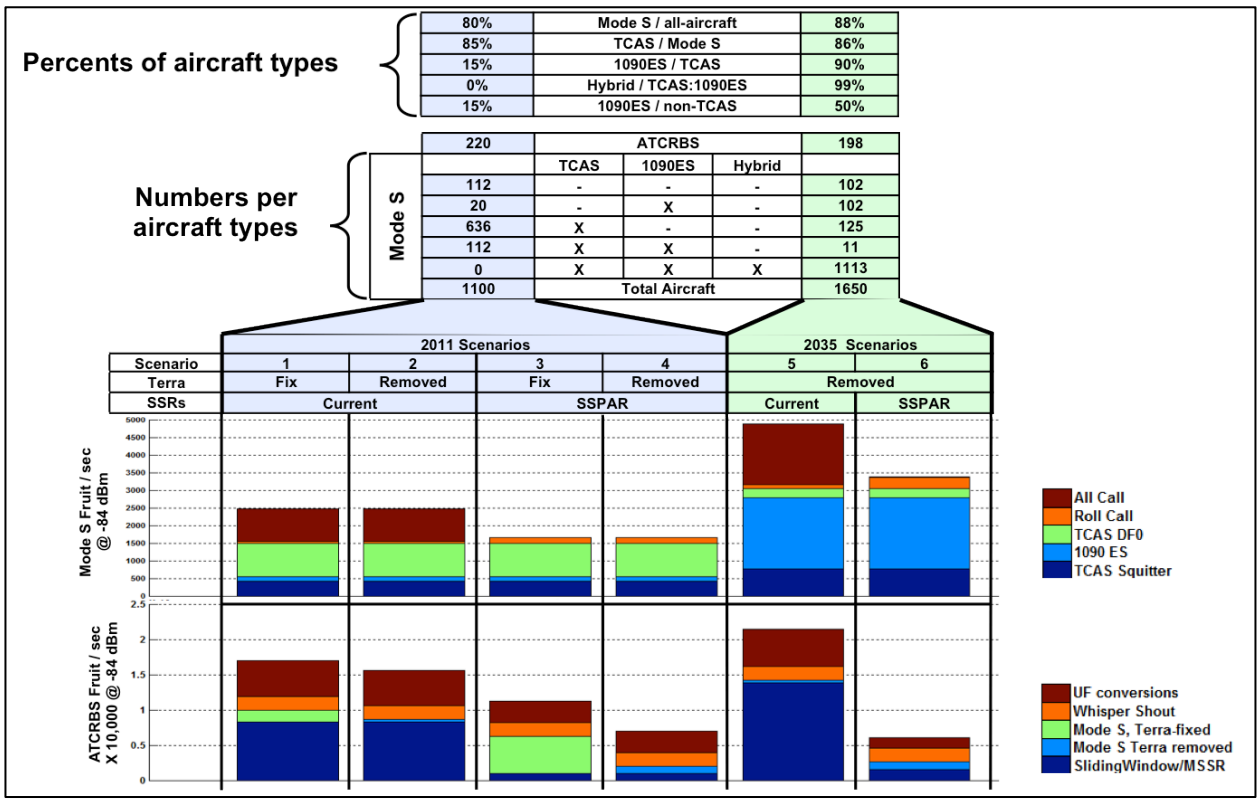

Figure 5-1. Modeled Mode-S and ATCRBS FRUIT rates for scenarios as described in the text. The upper portion of the figure breaks out the airplane equipage assumptions for the 2011 and 2035 scenarios.

Figure 5-2 shows the same modeled FRUIT activity by scenario, but in this figure the assumptions on secondary radar types and associated interrogation PRFs are shown explicitly.

In summary, SSPAR would provide a considerable reduction in Mode-S FRUIT, due to the elimination of All Calls and would also provide a considerable reduction in ATCBRS FRUIT, for the following reasons:

1. SSPAR would use a lower PRF in ATCRBS-mode than a Sliding Window ATCRBS;

2. SSPAR would eliminate All Call interrogations resulting in fewer UF Conversions; and

3. SSPAR would provide surveillance of Mode-S targets with Roll Calls instead of the ATCRBS interrogations used by Sliding Window ATCRBS and MSSR.

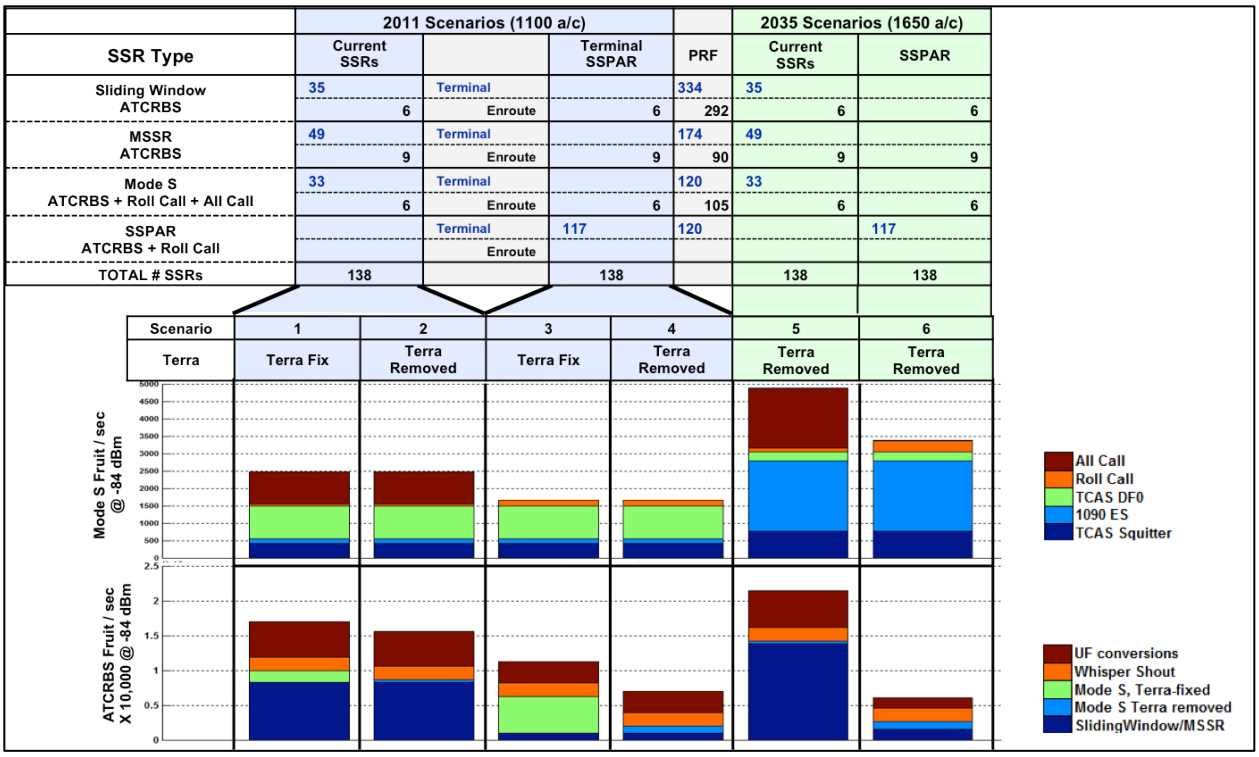

Figure 5-2. Modeled Mode-S and ATCRBS FRUIT rates for scenarios as described in the text. This is the same data as in Figure 5-1 but, here, the top portion of the figure breaks out the assumptions on the secondary radar types and associated interrogation PRFs for each of the scenarios.

6. SSPAR INTEGRATION WITH MULTIFUNCTION PHASED ARRAY RADAR (MPAR)

As noted in our concept overview, SSPAR may be deployed in conjunction with a next-generation electronically scanned primary radar (multifunction phased array radar or MPAR). In this configuration, both radars could be collaboratively managed to optimize aircraft and weather surveillance performance, reduce spectrum and timeline usage, and potentially reduce integrated system costs by downsizing requirements for the primary and/or secondary surveillance radar functions. In this section, we discuss very preliminary concepts for integrating SSPAR and MPAR surveillance functions.

6.1 SSPAR INTERROGATION RATE REDUCTION

One potential integration benefit would be to exploit the high-quality, three-dimensional surveillance provided by MPAR to reduce the rate at which SSPAR would interrogate ATCRBS and Mode-S targets. Table 6-1 compares Terminal MPAR's (TMPAR) estimated positioning accuracy with that of current secondary radars. (We assume that TMPAR would have a 3 dB beamwidth of approximately 1.3^{o} at broadside, and make the conservative assumption that at least a 10:1 beamsplit could be achieved using monopulse or similar techniques).

Table 6-1

Comparison of SSR Surveillance Capabilities with Terminal MPAR

	ATCRBS SSR	Monopulse SSR	Mode-S SSR	TMPAR
Range Accuracy	230 m	13 m	7 m	100 m
Bearing Accuracy	0.08^{o}	0.04^{o}	0.04^{o}	0.13^{o} broadside 0.2^{o} @ 45^{o}
Height Resolution	30 m	30 m	8 m	130 m @ 30 NM

From this comparison, it is plausible that TMPAR's surveillance capability would be sufficient to reduce the SSPAR interrogation rate for aircraft that are well separated laterally and/or in altitude. For example, SSPAR might interrogate each such aircraft only once every 14.4 seconds, thereby reducing the interrogation/reply rate by a factor of three relative to current rotating SSRs. TMPAR would be scheduled to provide the two intermediate position estimates. Note that for Mode-S aircraft, SSPAR could continue to listen to squittered altitude reports in between its roll-call interrogations so that high-resolution altitude surveillance would be maintained. Full analysis of viable approaches for utilizing TMPAR aircraft position measurements to reduce the SSPAR interrogation rate would require a reference level of safety analysis such as described in Thompson (2006).

6.2 MPAR AIRCRAFT TRACKING REQUIREMENTS RELIEF

An orthogonal SSPAR/MPAR integration concept would be to reduce MPAR track update requirements using scheduled SSPAR interrogations to "fill-in" surveillance reports for transponder-equipped aircraft. In terminal airspace, the TMPAR Notional Functional Requirements (NFR) document states that, for a maximum of 700 targets, TMPAR "must update reports on all aircraft targets already under track within the detection envelope at a threshold of at least once every 4.8 seconds, ±0.5 seconds, with an objective of once every second." Because TMPAR must also provide volumetric weather surveillance and perform a volumetric search for new, primary-only aircraft, this track update requirement may significantly affect TMPAR architecture choices and associated costs. Currently, the MPAR NFR document does not make a distinction between cooperative and non-cooperative targets in defining this update rate requirement. It would be reasonable to partition the requirement that "up to 700 aircraft be tracked" into cooperative and non-cooperative classes. This would allow for development of more efficient primary/secondary radar surveillance approaches.

6.3 CALIBRATION OF MPAR STORM HEIGHT ESTIMATES USING TRANSPONDER ALTITUDE REPORTS

Operational evaluations of Lincoln Laboratory's Corridor Integrated Weather System (CIWS) have indicated that radar-derived estimates of storm height can be utilized with high benefit in managing traffic flows through areas of convective weather (Robinson and Evans, 2006). Extensive analysis of aircraft trajectories in storm-impacted airspace has shown that the altitude difference between an aircraft and the "radar echo top" provided by CIWS is a strong predictor of the likelihood that the aircraft will deviate from its planned trajectory to avoid a storm. The relative altitude-difference threshold is about 5000′, suggesting that corresponding accuracy in the radar echo top estimate is needed.

As shown in Table 6-2, natural variation in the vertical gradient of atmospheric refractive index can result in significant changes in the effective "earth radius factor." Earth radius factor determines the curvature of radar beams versus slant range.

Table 6-2

Varations in Atmospheric Refractive Index Gradient

Condition	Refractive Index (N) Gradient (N/km)	Earth Radius Factor
Superrefraction	–157 to –79	2 to infinity
Normal	–70 to 0	1 to 2
"Standard Atmosphere"	–39	4/3
NEXRAD model	–27	1.21
Subrefraction	>0	<1

From Skolnik, Radar Handbook, 3rd Ed., 2008.

Corresponding variation in the beam height for TMPAR and the larger, long-range MPAR sensors are shown in Figure 6-1. It is seen that, for ranges exceeding about 100 km, variation in propagation conditions result in uncertainties of 5000′ or more as to the height of the center of the beam. This uncertainty could be significantly reduced using aircraft "targets of opportunity" that are under surveillance by both MPAR and SSPAR. The approach would be for MPAR to utilize monopulse to determine the apparent elevation angle of the aircraft with precision on the order of 0.1 degree. The barometric altitude reported to SSPAR via the transponder reply would then be used to correct the MPAR beam height estimate corresponding to this particular range, azimuth, and elevation combination. The procedure would be repeated for a large number of aircraft targets to continuously generate MPAR beam height calibrations spanning the surveillance volume.

Note that the beamwidth of TMPAR or MPAR is significant in relation to these propagation-induced height uncertainties, particularly at shorter ranges. Because of the sharp vertical reflectivity gradient at the upper edge of convective storms, however, MPAR will be able to achieve "sub-beamwidth" resolution of the radar echo top by adaptively scanning the beam in elevation angle through the storm top. The sharp cutoff in returned power as the lower edge of the beam scans above the echo top will provide a high-resolution estimate for radar echo top.

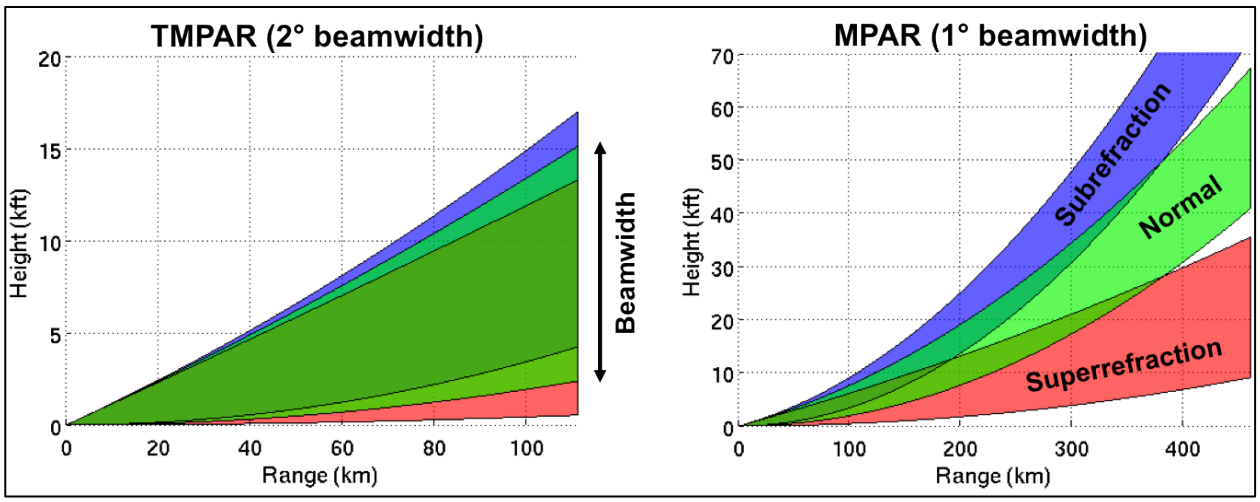

Figure 6-1. Terminal and Full-Scale MPAR beam height versus range for differing propagation conditions.

7. SUMMARY AND RECOMMENDATIONS

The SSPAR operational concept and preliminary performance analysis presented in this report are very encouraging. Relative to current, rotating secondary surveillance radars, SSPAR is likely to have lower recurring acquisition and life-cycle maintenance cost, will maintain the positional accuracy achieved by MSSR or Mode-S and will substantially reduce 1030/1090 MHz spectrum usage. Owing to its capability to listen continuously in all directions to squitters from Mode-S/ADS-B–equipped aircraft, SSPAR can operate in modes not realizable with a rotating SSR. For example, SSPAR can serve as an ADS-B ground station when GPS is in service and can maintain the ADS-B once-per-second update rate during any temporary GPS outage. Thus airspace capacity would not be compromised during such outages. The SSPAR system architecture is straightforward and we showed that its component subsystems can be developed using commercially available technology.

The key challenge for fully validating the SSPAR concept is more comprehensive analysis of the array signal and data processing algorithms. Particularly, in future, high-density airspace the number of transponder replies reaching the array at any given instant will be large. Robust transponder reply detection, direction estimation and signal decoding – built on the Adaptive Event Processing (AEP) technique described previously – must be fully developed and demonstrated in dense FRUIT environments.

We recommend the following high-level roadmap for SSPAR development.

(i) Continued processing algorithm development using the FRUIT model-based Monte Carlo simulations described in Section 3. A key processing algorithm extension will be the development and validation of time-varying SSPAR receive beamformers to support the decoding of long-duration replies from Mode-S/ADS-B transponders. In addition, the performance trade-space for ATCRBS interrogation must be further analyzed to understand the optimal combination of interrogation directivity, Whisper Shout transmission, and array processing complexity.

(ii) Data collection in a high FRUIT environment using an antenna array with characteristics at least similar to the SSPAR array concept described in this report. Signals from each array channel would be recorded and analyzed off-line to validate the assumptions of the FRUIT model and to demonstrate that the SSPAR processing techniques achieve desired levels of performance.

(iii) Development and evaluation of a SSPAR prototype, including real-time interrogation and reply processing to fully demonstrate concepts of operation and surveillance capability. The prototype development, integration, and test could be performed by means of government/industry collaboration so that at completion of the prototype evaluation, the

government would be in a position to move forward with an industry contract for SSPAR manufacture and deployment.

We are confident that, given appropriate resources, the above development roadmap could be accomplished in a period of three years.

REFERENCES

W.H. Harman and M.L. Wood, "Triangle TCAS Antenna," Project Report ATC-380, MIT Lincoln Laboratory, Lexington, MA, March 2011.

G.F. Hatke, "Superresolution Source Location with Planar Arrays," MIT Lincoln Laboratory Journal, Volume 10, Number 2, 1997.

M. Weber, J. Herd, J. Cho, and G. Jones, "Multifunction Phased Array Radar (MPAR): Achieving Next Generation Surveillance and Weather Radar Capability," Journal of Air Traffic Control, Vol. 55, No. 3, Fall 2013.

K.W. Forsythe, "Utilizing waveform features for adaptive beamforming and direction finding with narrowband signals," Lincoln Laboratory Journal, 10 (2), 99–126, 1997.

W.H. Harman, "Effects of RF Power Deviations on BCAS Link Reliability," Project Report ATC-76, Lincoln Laboratory (7 June 1977).

Stanley R. Jones, "Analytic Model for 1090 MHz Extended Squitter ADS-B Bench Test Evaluation," MITRE CAASD, September 2008.

"Investigation of spectrum impact of equipping unmanned aircraft with 1030 MHz transmitters for collision avoidance," MIT Lincoln Laboratory, 6 June 2013.

S.D. Thompson and J.M. Flavin, "Surveillance Accuracy Requirements in Support of Separation Services," MIT Lincoln Laboratory Journal, Volume 16, Number 1, 2006.

M. Robinson and J.E. Evans, "Assessment of Air Traffic Control Productivity Enhancements from the Corridor Integrated Weather System (CIWS), Executive Summary," Project Report ATC-325-1, MIT Lincoln Laboratory, Lexington, MA, 2006.

This page intentionally left blank.